Inorg. Chem. **2007**, *46*, 4523–4529

Inorganic Chemistry Article

Synthesis, Structure, and Properties of $BaAl_2Si_2$

Cathie L. Condron,† Håkon Hope,† Paula M. B. Piccoli,‡ Arthur J. Schultz,‡ and Susan M. Kauzlarich*,†

Department of Chemistry, One Shields Avenue, University of California, Davis, California 95616, and Intense Pulsed Neutron Source, Argonne National Laboratory, Argonne, Illinois 60439-4814

Received January 16, 2007

Single crystals of $BaAl_2Si_2$ were grown from an Al molten flux and characterized using single-crystal X-ray diffraction at 10 and 90 K and neutron diffraction at room temperature. $BaAl_2Si_2$ crystallizes with the α-$BaCu_2S_2$ structure type (*Pnma*), is isostructural with α-$BaAl_2Ge_2$, and is an open 3D framework compound, where Al and Si form a covalent cagelike network with Ba^{2+} cations residing in the cages. $BaAl_2Si_2$ has a unit cell of a = 10.070(3) Å, b = 4.234(1) Å, and c = 10.866(3) Å, as determined by room-temperature single-crystal neutron diffraction (R1 = 0.0533, wR2 = 0.1034). The structure as determined by single-crystal neutron and X-ray diffraction (10 and 90 K) indicates that $BaAl_2Si_2$ (*Pnma*) is strictly isostructural to other (α)-$BaCu_2S_2$-type structures, requiring site specificity for Al and Si. Unlike $BaAl_2Ge_2$, no evidence for an α to β ($BaZn_2P_2$-type, *I*4/*mmm*) phase transition was observed. This compound shows metallic electronic resistivity and Pauli paramagnetic behavior.

Introduction

The unexpected discovery of superconductivity at T_c = 39 K in MgB_2[1] has fueled speculation that many interesting physical properties, including superconductivity, are favored when electron mobility is limited to fewer than three dimensions.[2] This speculation attracted significant attention to the AlB_2 family of compounds, including ternary silicides $MX_{2-x}Si_x$, where M = Ca, Sr, Ba and X = Ga, Al, that exhibit T_c values ranging from 2 to 7.8 K.[3−7] In addition to superconductivity, 2-D aluminum silicon phases are also being explored for their potential as hydrogen-storage materials.[8]

3D Al−Si systems, such as clathrate phases, also have unique and important properties and are being studied for their potential application in thermoelectric materials.[9−11] Indeed, these lightweight, low-density compounds may provide excellent high-temperature thermoelectric materials for transportation and waste-heat utilization.

The majority of AM_2X_2 compounds crystallize with the $ThCr_2Si_2$ structure type, space group *I*4/*mmm*.[12] The second most abundant crystal structure that the AM_2X_2 compounds form is the $CaAl_2Si_2$ structure type, space group $P\bar{3}m1$.[13] The formation of the $CaAl_2Si_2$ structure type is tied to specific conditions, where the number of valence electrons should not exceed 16.[14−16] Exceptions to this rule are found in the trivalent rare-earth metals $LnAl_2X_2$ (Ln = rare earth, X = Si, Ge) with 17 electrons,[17,18] which are stabilized by

* To whom correspondence should be addressed. E-mail: smkauzlarich@ucdavis.edu.
† University of California.
‡ Argonne National Laboratory.

(1) Nagamatsu, J.; Nakagawa, N.; Muranka, T.; Zenitani, Y.; Akimitsu, J. *Nature (London)* **2001**, *63*, 410.
(2) King, R. B. In *Concepts in Chemistry*; Rouvray, D. H., Ed.; Wiley: New York, 1997.
(3) Lorenz, B.; Cmaidalka, J.; Meng, R. L.; Chu, C. W. *Phys. Rev. B* **2003**, *68*, 014512.
(4) Imai, M.; Abe, E.; Ye, J.; Nishida, K.; Kimura, T.; Honma, K.; Abe, H.; Kitazawa, H. *Phys. Rev. Lett.* **2001**, *87*, 077003.
(5) Imai, M.; Nishida, K.; Kimura, N.; Abe, H. *Appl. Phys. Lett.* **2002**, *80*, 1019.
(6) Imai, M.; Nishida, K.; Kimura, T.; Abe, H. *Physica C (Amsterdam)* **2002**, *377*, 96.
(7) Imai, M.; Nishida, K.; Kimura, T.; Kitazawa, H.; Abe, H.; Kito, H.; Yoshii, K. *Physica C (Amsterdam)* **2002**, *382*, 361.
(8) Bjoerling, T.; Noreus, D.; Jansson, K.; Andersson, M.; Leonova, E.; Eden, M.; Haalenius, U.; Haeussermann, U. *Angew. Chem., Int. Ed.* **2005**, *44*, 7269.
(9) Mudryk, Y.; Rogl, P.; Paul, C.; Berger, S.; Bauer, E.; Hilscher, G.; Godart, C.; Noel, H. *J. Phys.: Condens. Matter* **2002**, *14*, 7991.
(10) Mudryk, Y.; Rogl, P.; Paul, C.; Berger, S.; Bauer, E.; Hilscher, G.; Godart, C.; Noel, H.; Saccone, A.; Ferro, R. *Physica B (Amsterdam)* **2003**, *328*, 44.
(11) Condron, C. L.; Porter, R.; Guo, T.; Kauzlarich, S. M. *Inorg. Chem.* **2005**, *44*, 9185.
(12) Ban, Z.; Sikirica, M. *Acta Crystallogr.* **1965**, *18*, 594.
(13) Gladyshevskii, E. J.; Kripyakevich, P. I.; Bodak, O. I. *Ukr. Fiz. Zh.* **1967**, *13*, 447.
(14) Klufers, P.; Mewis, A. *Z. Naturforsch., B: Anorg. Chem., Org. Chem.* **1977**, *32*, 753.
(15) Klufers, P.; Mewis, A. *Z. Kristallogr.* **1984**, *169*, 135.
(16) Artmann, A.; Mewis, A. *Z. Anorg. Allg. Chem.* **1996**, *622*, 679.
(17) Zarechnyuk, O. S.; Muravyova, E. I.; Gladyshevskii, E. J. *Dopov. Akad. Nauk. Ukr. RSR, Ser. A: Fiz.−Tekh. Mat. Nauk* **1970**, *32*, 753.
(18) Nesper, R.; Schnering, v. H. G.; Curda, J. *Z. Naturforsch., B: Chem. Sci.* **1987**, *37*, 1514.

10.1021/ic070078h CCC: $37.00

Published on Web 05/01/2007

the small electronegativity differences of the atoms in the M_2X_2 slabs closing the gap between the valence and conduction band.[19−21]

Less common are compounds that crystallize with the α-$BaCu_2S_2$ structure type, space group *Pnma*,[22,23] of which α-$BaCu_2Se_2$, $BaZn_2As_2$, $BaZn_2Sb_2$, α-$ThNi_2P_2$,[24] α-$BaCu_2Te_2$,[25] and $BaAl_2Ge_2$[26] are representatives. Recently, the phase $EuIn_2P_2$, which exhibits a new structure type, has been added to the AM_2X_2 family.[27] $EuIn_2P_2$ crystallizes in the hexagonal space group $P6_3/mmc$ and exhibits colossal magnetoresistance of up to −398%. The discovery of several new phases in the AM_2X_2 family that display exciting and unusual properties exemplifies the importance of exploratory research in the field of solid-state and materials science.

While we were investigating the optimal growth conditions for the $Ba_8Al_{16}Si_{30}$ type-I clathrate phase, $BaAl_2Si_2$ was found as a secondary phase.[11,28−30] $BaAl_2Si_2$ is part of the large family of AM_2X_2 compounds (A = rare and alkaline earth elements, M = metal, and X = main group 3−6 elements).[14−16] Two structure types of $BaAl_2Si_2$ have been previously reported, β (*I*4/*mmm*), prepared at high pressure, and α (*Cmcm*), prepared by annealing an arc-melted sample on stoichiometry.[31] This paper presents a new modification of $BaAl_2Si_2$, the α-$BaCu_2S_2$ structure type (*Pnma*), which is isostructural with $BaAl_2Ge_2$.[26] A structure view of this compound has been presented in a paper on $EuGa_2Ge_4$ by Carrillo-Cabrera et al.;[32] however, no details concerning the synthesis, structure, or property measurements were presented. $BaAl_2Ge_2$ exists in two modifications: α, a low-temperature phase (α-$BaCu_2S_2$ structure type, space group *Pnma*), and β, a high-temperature phase ($BaZn_2P_2$ structure type, space group *I*4/*mmm*, a variant of the $ThCr_2Si_2$ structure type). There is a reversible α−β phase transition observed for $BaAl_2Ge_2$.[26] In the present paper, the synthesis, crystal structure, and electronic transport properties are presented and discussed. A single-crystal X-ray data set measured with the crystal at 90 K provided a strong indication of site ordering for Al and Si. Subsequent 10 K X-ray data, as well as room-temperature neutron data, provided substantial strengthening of this indication. Each data set alone allowed unambiguous site assignment, assuming a site-ordered structure, for Al and Si.

(19) Kranenberg, C.; Johrendt, D.; Mewis, A. *Z. Anorg. Allg. Chem.* **1999**, *625*, 1787.
(20) Kranenberg, C.; Johrendt, D.; Mewis, A. *Solid State Sci*. **2002**, *4*, 261.
(21) Kranenberg, C.; Johrendt, D.; Mewis, A.; Pottgen, R.; Kotzyba, G.; Rosenhahn, C.; Mosel, B. D. *Solid State Sci*. **2000**, *2*, 215.
(22) Iglesia, J. E.; Pachali, K. E.; Steinfink, H. *J. Solid State Chem.* **1974**, *9*, 6.
(23) Huster, J.; Bronger, W. *Z. Anorg. Allg. Chem.* **1999**, *625*, 2003.
(24) Albering, J.; Jeitschko, W. *Z. Naturforsch.* **1999**, *49b*, 1074.
(25) Wang, C.; DeSalvo, F. J. *J. Solid State Chem.* **2001**, *156*, 44.
(26) Leoni, S.; Carrillo-Cabrera, W.; Schnelle, W.; Grin, Y. *Solid State Sci.* **2003**, *5*, 139.
(27) Jiang, J.; Kauzlarich, S. M. *Chem. Mater.* **2006**, *18*, 435.
(28) Condron, C. L.; Gascoin, F.; Snyder, G. J.; Kauzlarich, S. M. *Chem. Mater.* **2006**, *18*, 4939.
(29) Condron, C. L.; Kauzlarich, S. M.; Nolas, G. S. *Inorg. Chem.* **2007**, *46*, 2556.
(30) Condron, C. L.; Martin, J.; Nolas, G. S.; Piccoli, P. M.; Shultz, A. J.; Kauzlarich, S. M. *Inorg. Chem.* **2006**, *45*, 9381.
(31) Yamanaki, S.; Kajiyama, M.; Sivakumar, S. N.; Fukuoka, H. *High Pressure Res.* **2004**, *24*, 481.
(32) Carrillo-Cabrera, W.; Paschen, S.; Grin, Y. *J. Alloys Compd.* **2002**, *333*, 4.

Experimental Section

Synthesis. Starting materials for the preparation of $BaAl_2Si_2$ were Ba (Johnson Matthey, 99.9%), Si (AESAR, 99.999%), and Al (Matheson Colemen and Bell 99.6%). All preparations were performed in a nitrogen-filled dry box with water levels of less than 1 ppm. Single-crystal samples were grown using the high-temperature metallic solution growth method,[33] with an optimized atomic ratio of the elements 1 Ba/2 Si/10 Al scaled to 1 g of Al. The elements were layered into a 2 mL alumina crucible and placed into a fused silica tube. A plug of SiO_2 wool was then placed on top of the reaction crucible. The fused silica tube was subsequently sealed under 0.2 atm of argon. The reaction vessel was placed upright in a box furnace and heated from room temperature to 1000 °C over a period of 4 h, held at 1000 °C for 10 h, and slowly cooled at 1 °C h^{-1} to 800 °C. Flux reactions were removed from the furnace at 800 °C and the excess liquid was decanted. Single-crystal samples were found to be stable in air, water, and alcohol. However, this phase dissolves vigorously in dilute acid and base solutions. We also note that a small amount of $BaAl_4$ is present in this reaction as a powder.

Microprobe Analysis. Single crystals of $BaAl_2Si_2$ were obtained from several different reactions, mounted in epoxy, and polished for subsequent analyses. The samples were then placed in a Cameca SX-100 electron microprobe equipped with five wavelength-dispersive spectrometers. The microprobe was operated at 10 nA current with a 20 keV accelerating potential. Net elemental intensities for Al and Si were determined with respect to pure elemental calibration standards. $BaAl_{3.54}Si_{0.41}$ was used as a standard to determine the net elemental intensities for Ba. The totals for all analyses were 100%. The elemental stoichiometry was quantitatively determined to be $Ba_{1.02(2)}Al_{1.99(2)}Si_{1.99(2)}$. The compositions were homogeneous within one crystal and, within standard uncertainty, identical compared with crystals selected at random from different reactions.

X-ray Powder Diffraction. X-ray powder diffraction data for $BaAl_2Si_2$ were collected with a Scintag PAD-V employing Cu Kα radiation. Data acquisition was performed with WinAcq software. Powder diffraction data were calculated for the two published phases of $BaAl_2Si_2$ (*Cmcm*, *I*4/*mmm*)[31] using the program Crystal Diffract.[34]

Single-Crystal X-ray Diffraction. A suitable, highly reflective crystal was selected, cut to the dimensions 0.09 × 0.12 × 0.15 mm^3, and mounted on a glass fiber. Data were collected using a Bruker APEX 2 CCD diffractometer equipped with a Cryo Industries of America CRYOCOOL LHe device for the 10 K data and a CRYOCOOL LN2 device for the 90 K data, employing graphite-monochromated Mo Kα radiation (λ = 0.71073 Å). The temperature was measured with a calibrated Si diode placed at the crystal position before and after data collection. Lorentz and polarization corrections were applied using the SAINT program; absorption corrections were based on fitting a function to the empirical transmission surface as sampled by multiple equivalent reflections (program SADABS).[35]

Single-Crystal Neutron Diffraction. Single-crystal neutron diffraction data were collected using the SCD instrument at the Intense Pulsed Neutron Source, Argonne National Laboratory.[36−38]

(33) Canfield, P. C.; Fisk, Z. *Philos. Mag. B* **1992**, *65*, 1117−1123.
(34) *CrystalDiffract*; CrystalMaker Software Limited: Oxfordshire, U.K., 2006.
(35) Sheldrick, G. M. *SADABS*; Bruker AXS: Madison, WI, 1999.

Table 1. Crystal Data and Structure Refinement for $BaAl_2Si_2$

temp (K)	298 (neutron)	90 (X-ray)	10 (X-ray)
space group	*Pnma*	*Pnma*	*Pnma*
lattice params (Å)	$a = 10.070(3)$	$a = 10.0807(5)$	$a = 10.0736(9)$
	$b = 4.234(1)$	$b = 4.227(2)$	$b = 4.2255(4)$
	$c = 10.866(3)$	$c = 10.874(5)$	$c = 10.8653(9)$
vol. (Å^3)	463.3(2)	463.41(4)	462.49(7)
Z	4	4	4
density (calcd) (Mg/m^3)	3.548	3.660	3.554
abs coeff (mm^{-1})	$0.0093 + 0.0009\lambda$	9.260	9.278
θ range (deg)	~26−71	3.75−31.48	2.76−31.49
wavelength	0.5−5.0 Å	Mo Kα	Mo Kα
independent reflns	1453	856	853
data/restraints/params	1453/0/35	760/0/32	853/0/32
GOF on F^2	1.185	1.055	1.169
final R indices [$I > 2\sigma(I)$][a]	R1 = 0.0533	R1 = 0.0137	R1 = 0.0126
	wR2 = 0.1034	wR2 = 0.0382	wR2 = 0.0255
R indices (all data)	R1 = 0.0604	R1 = 0.0143	R1 = 0.0145
	wR2 = 0.1060	wR2 = 0.0382	wR2 = 0.0267
extinction coeff	0.000143(4)	0.0011(4)	0.0000(2)
largest diff peak and hole (neutron, fm Å^{-3}; X-ray, e Å^{-3})	0.388 and −0.600	1.014 and −0.717	0.625 and −0.482

[a] $R1 = [\sum||F_o| - |F_c||]/\sum|F_o|$; $wR2 = \{[\sum w[(F_o)^2 - (F_c)^2]^2]\}^{1/2}$; $w^{-1} = [\sigma^2(F_o) + (0.0471P)^2 + (0.5945P)]$, where $P = [\max(F_o^2,0) + 2F_c^2/_3]$.

The room-temperature measurement was carried out on a crystal of $BaAl_2Si_2$ with approximate dimensions of 1 × 1.5 × 3 mm^3 and a weight of 0.0229 g. It was glued to an aluminum pin. The SCD beam line employs a white beam spallation source with a diffractometer equipped with two position-sensitive area detectors. Details of the data collection and analysis procedures have been published previously.[39] The GSAS software package was used for structural analysis.[40] The atomic positions from the X-ray diffraction structure were used as a starting point in the refinement. The refinement was based on F^2 for reflections with a minimum d spacing of 0.71 Å. All atoms were refined with anisotropic displacement parameters. Data collection and refinement parameters are summarized in Table 1.

TG/DSC. A Netzsch Thermal Analysis STA 409 STA was used to evaluate the thermal properties of $BaAl_2Si_2$ between 25 and 1500 °C. After a baseline was established, several crystals ground into a powder (40−60 mg) were placed in alumina crucibles and heated under argon at 10 K min^{-1} with an acquisition rate of 4 points K^{-1}. The results were verified for several reactions.

Electronic Transport Measurement. DC magnetization data were collected using a Quantum Design MPMS superconducting quantum interference device (SQUID) magnetometer with a 7 T superconducting magnet. Temperature-dependent magnetization measurements of $BaAl_2Si_2$ were obtained by using a 22.2 mg clean single crystal held in a straw. The temperature-dependent data were obtained by measurement of the zero-field-cooled (ZFC) magnetization from 2 to 300 K and field-cooled (FC) magnetization from 2 to 300 K in an applied magnetic field of 1 T.

(36) Schultz, A. J. *Trans. Am. Crystallogr. Assoc.* **1987**, *23*, 61.
(37) Schultz, A. J.; Teller, R. G.; Williams, J. M.; Lukehart, C. M. *J. Am. Chem. Soc.* **1984**, *106*, 999.
(38) Schultz, A. J.; Van Derveer, D. G.; Parker, D. W.; Baldwin, J. E. *Acta Crystallogr. C* **1990**, *46*, 276.
(39) Jacobson, R. A. *J. Appl. Phys.* **1986**, *19*, 283.
(40) Larson, A. C.; Von Dreele, R. B. *General Structure Analysis System (GSAS)*; Los Alamos National Laboratory Report LAUR 86-748; Los Alamos National Laboratory: Los Alamos, NM, 2004.

Table 2. Atomic Coordinates and Equivalent Isotropic Displacement Parameters (U_{eq})[a] for $BaAl_2Si_2$

atom	site	x	y	z	U_{eq} (Å^2)	occupancy
			298 K (neutron)			
Ba	4c	0.747779(12)	1/4	0.67422(10)	0.0104(3)	1
Si(1)	4c	0.35462(15)	1/4	0.54105(13)	0.0093(4)	1
Si(2)	4c	0.97645(16)	1/4	0.34407(13)	0.0098(4)	1
Al(1)	4c	0.54168(18)	1/4	0.38073(16)	0.0103(4)	1
Al(2)	4c	0.10168(18)	1/4	0.54776(15)	0.0095(4)	1
			90 K (X-ray)			
Ba	4c	0.747892(10)	1/4	0.674498(11)	0.00444(7)	1
Si(1)	4c	0.35447(6)	1/4	0.54111(5)	0.00431(11)	1
Si(2)	4c	0.97626(6)	1/4	0.34389(5)	0.00403(12)	1
Al(1)	4c	0.54178(6)	1/4	0.38114(6)	0.00490(13)	1
Al(2)	4c	0.10157(7)	1/4	0.54773(6)	0.00496(13)	1
			10 K (X-ray)			
Ba	4c	0.747873(11)	1/4	0.674526(11)	0.00243(5)	1
Si(1)	4c	0.35432(6)	1/4	0.54103(5)	0.00352(11)	1
Si(2)	4c	0.97624(6)	1/4	0.34377 (5)	0.00317(11)	1
Al(1)	4c	0.54180(6)	1/4	0.38114(6)	0.00373(12)	1
Al(2)	4c	0.10130(6)	1/4	0.54776(6)	0.00389(13)	1

[a] U_{eq} is defined as one-third of the trace of the orthogonalized U^{ij} tensor.

Resistivity of $BaAl_2Si_2$ was measured on a crystal of 1.2 × 0.3 × 0.7 mm^3 dimensions. Platinum wires were attached to the crystal with Epo−Tex silver epoxy. The resistivity temperature dependence of $BaAl_2Si_2$ was measured using the four-probe method over the temperature range of 300 to 2 K using a Quantum Design PPMS (physical properties measurement system).

Results and Discussion

Single crystals of $BaAl_2Si_2$ were prepared via an Al flux reaction. Microprobe analysis was consistent with the stoichiometry as written. Single-crystal X-ray and neutron diffraction confirms that $BaAl_2Si_2$ crystallizes with the α-$BaCu_2S_2$ structure (space group *Pnma*).[22,23] The results are summarized in Table 1, and selected bond lengths are compiled in Table 2. This structure type can be viewed as a simpler form of the clathrate-I structure type.[26] Clathrate type-I structures, such as $BaAl_{16}Si_{30}$,[28−30] show mixed site occupancy for the Al and Si atoms in the framework. In the case of $BaAl_2Ge_2$, X-ray diffraction clearly identifies the Al and Ge sites, and there is no evidence for mixed occupancy. Many Al−Si clathrates and other phases show mixed site occupancy; therefore, X-ray diffraction may not be sufficient to identify whether or not the structure has site preferences or mixed occupancy. In the recent report on two new modifications of $BaAl_2Si_2$, β (*I*4/*mmm*) and α (*Cmcm*), the Al and Si sites were tentatively assigned to the same sites as the Al and Ge in α-$BaAl_2Ge_2$.[31] The X-ray scattering factors for Al and Si differ by about 7−14% for $2\theta = 0-60°$ for Mo Kα radiation. In cases where there is no mixed occupancy, this difference is sufficient to make a clear distinction between Al and Si, given reasonable data quality. The present case, in principle, requires a distinction to be made between mixed Al−Si occupancy and site specificity.

A number of models were tested for the 90 K X-ray data set. Among these were Ba plus all Al and Ba plus all Si. The results of each of these models strongly pointed toward Al and Si occupying separate sites. Either Al at the Si sites or Si at the Al sites resulted in anomalous values for the atomic displacement parameters. For example, with Al and Si occupying individual sites, the isotropic *U* values are in the range of 0.004−0.005 Å^2. With the Si sites occupied by Al, the *U* values for Si were below 0.002 Å^2. A refinement with the occupancies of Al and Si as adjustable variables gave 100% occupancy (within 3σ) for each site, with a standard uncertainty of about 4% for each occupancy. If the Al sites had been partially occupied by Si, this should have been indicated by an Al "occupancy" of over 100%. There was no such indication.

The lowering of the temperature to 10 K will diminish the thermal motion of atoms. We expected this to result in a sharper distinction between Al and Si. Calculations based on the models used for the 90 K data bear this out. Indications from atomic displacement values were particularly strong. With Al and Si assigned full individual occupancies, the isotropic *U* values were all between 0.003 and 0.004 Å^2. With the Si positions occupied by Al, the Si *U* values refined to near zero, while for Al, they remained normal. Refinement of individual occupancies resulted in 100% occupancy for all atoms, within 3 standard uncertainties. The standard uncertainties, at 3−3.5%, were somewhat lower than for the 90 K data.

The absence of any indication of mixed occupancy resulting from the two X-ray studies provides strong evidence for a site-specific structure. To reduce any uncertainty, we also performed a neutron diffraction study. In neutron diffraction, the difference in scattering power between Al and Si is a constant ∼18% at all values of (sin θ)/λ, in comparison to a range of ∼7−14% in X-ray diffraction. As expected, the distinction between Al and Si with neutron data is even sharper than with the X-ray data. All occupancies refined to 100%, within less than 2 standard uncertainties. The standard uncertainty in individual occupancies is about 1.2%. From these results it is not possible to completely exclude mixed occupancy, but it is certain that it is very low. The three structure determinations all give the same result in that the most likely distribution is one of Al and Si occupying separate sites.

The examination of other representatives of the α-$BaCu_2S_2$ structure type (space group *Pnma*),[22,23] such as α-$BaCu_2Se_2$, $BaZn_2As_2$, $BaZn_2Sb_2$, α-$ThNi_2P_2$,[24] α-$BaCu_2Te_2$,[25] and $BaAl_2Ge_2$,[26] show that they are strictly isostructural. In each case, the metals and the main-group elements occupy corresponding positions. We propose that this is a defining characteristic of this structure type. It seems likely that the underlying cause is a common bonding scheme. The site specificity is thus a requirement for this structure type.

As mentioned above, we describe a new modification of $BaAl_2Si_2$. The structure assignment agrees with that reported by Carrillo-Cabrera et al.[32] A modification of $BaAl_2Si_2$ has been reported to crystallize in a variation of the α-$BaAl_2Ge_2$ structure, in the *Cmcm* space group, and also in a high-pressure modification that crystallizes with the $ThCr_2Si_2$ (*I*4/*mmm*) structure.[31] The *Cmcm* modification was reported as prepared by arc melting with subsequent annealing at 1200 °C for 1 day, then cooling to 800 °C over a period of 2 days, followed by cooling to room temperature

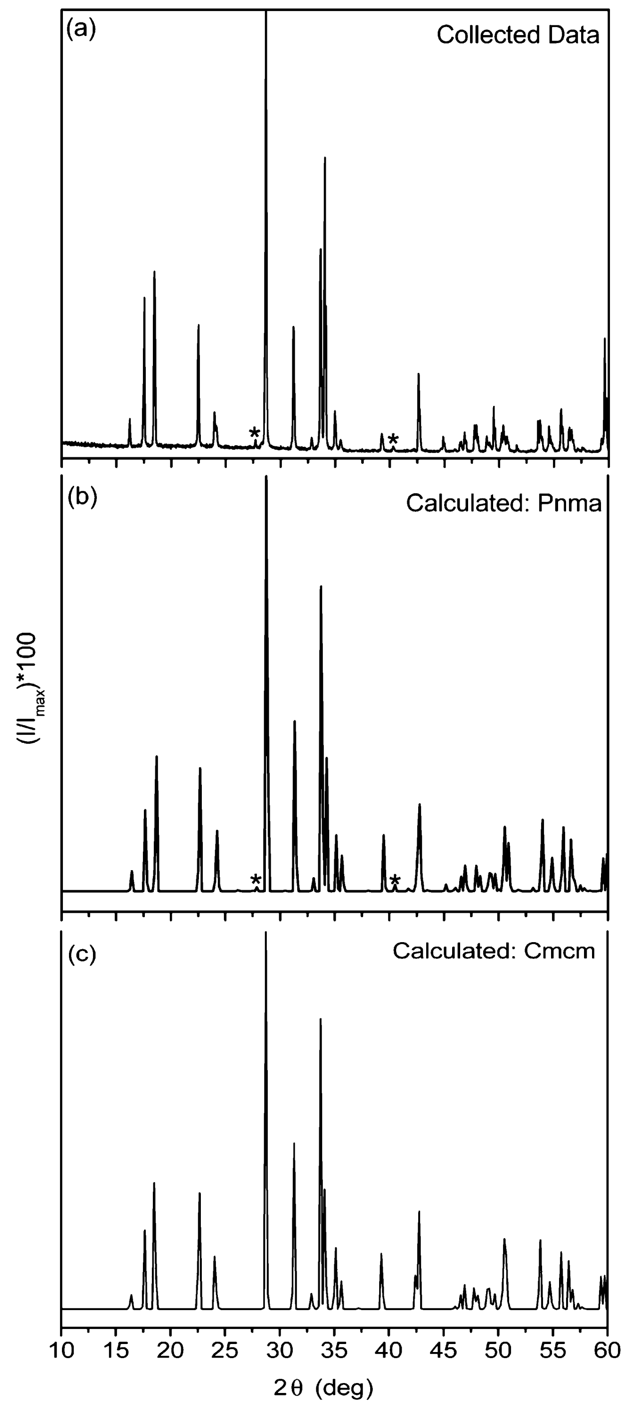

Figure 1. Experimental and calculated X-ray powder diffraction pattern for (a) $BaAl_2Si_2$ single crystals ground into a powder and calculated X-ray powder diffraction patterns for (b) $BaAl_2Si_2$ space group *Pnma*[42] and (c) $BaAl_2Si_2$ space group *Cmcm*.[42] Intensities are normalized to 100 for comparison.

over a period of 2 days.[32] This *Cmcm* structure is a variant of the α-$BaAl_2Ge_2$ structure type. We obtained the *Pnma* phase, reported herein, from an aluminum flux heated over 4 h to 1000 °C, for 10 h, and cooling to 800 °C at a rate of 3° hr^{-1}. The crystals were obtained by decanting the flux at 800 °C. Since different synthetic conditions resulted in different modifications, the preparation method is apparently important. Alternatively, we can propose that the structure transforms in the following manner *I*4/*mmm* → *Cmcm* →

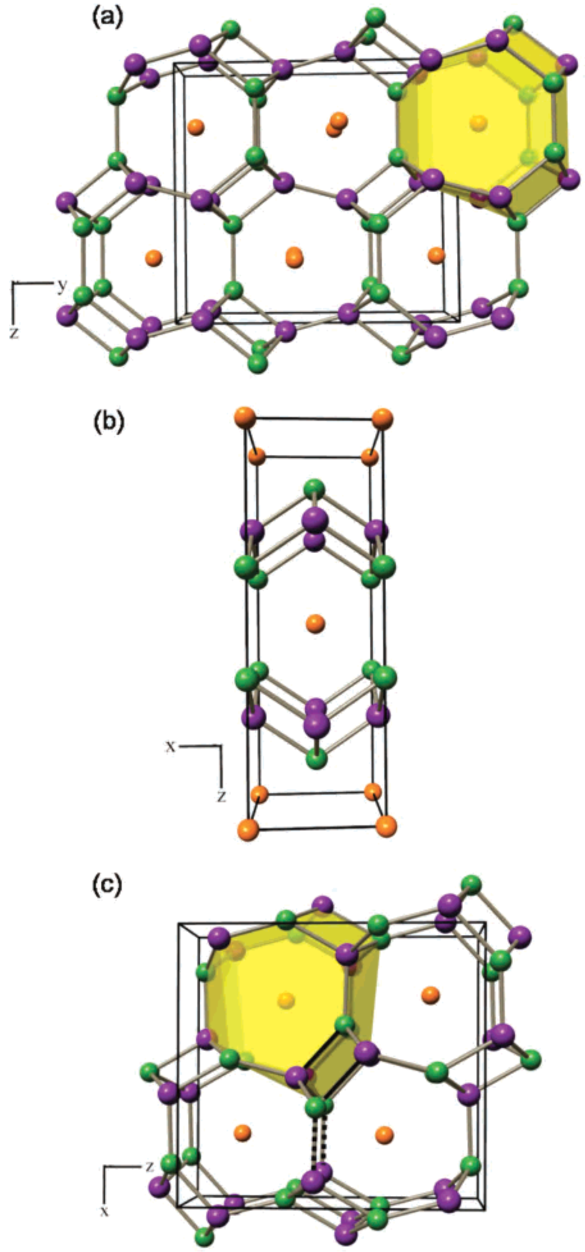

Figure 2. Illustration of unit cell for $BaAl_2Si_2$ in the space groups (a) *Cmcm*, (b) *I*4/*mmm*, and (c) *Pnma* (Ba = orange, Si = green, Al = purple). The crystal structures were generated by Balls and Sticks.[43]

Pnma. This is reasonable, given that the dimorphism found in α-$BaCu_2Si_2$[23] and α-$BaAl_2Ge_2$[26] similarly corresponds to a transformation from the high-temperature *I*4/*mmm* space group to the low-temperature *Pnma* space group. However, there is no evidence of such transition in our TGA/DSC data, which will be discussed latter. It is also important to mention that the differences in structure between the *Pnma* and *Cmcm* modifications are very small. Therefore, although there is no indication that the space group *Pnma* from our single-crystal X-ray diffraction experiments is incorrect, X-ray powder diffraction was used to ensure that the assignment was absolutely correct as each space group will have a different "fingerprint." The experimental X-ray powder diffraction pattern for $BaAl_2Si_2$ (*Pnma*) is shown in Figure 1a. For comparison, the calculated powder patterns for $BaAl_2Si_2$ (*Pnma*) and $BaAl_2Si_2$ (*Cmcm*) are shown in Figure 1b and 1c, respectively. The patterns are similar for *Pnma* and *Cmcm*; however, the small peaks indicated with an asterisk (*) confirm the assignment of *Pnma* as correct for the $BaAl_2Si_2$ modification of the phase obtained from Al flux. There are slight intensity differences between the measured and calculated X-ray powder diffraction patterns, likely due to preferred orientation.

Table 3. Interatomic Distances (Å) and Bond Angles (deg) for $BaAl_2Si_2$

	298 K (neutron)	90 K (X-ray)	10 K (X-ray)
Al1−2Si1	2.5088(13)	2.5053(5)	2.5048(5)
Al1−Si1	2.566(2)	2.5674(9)	2.5661(9)
Al1−Si2	2.530(2)	2.5346(8)	2.5313(9)
Al2−2Si2	2.5446(13)	2.5440(5)	2.5423(5)
Al2−Si2	2.547(2)	2.5512(9)	2.5494(9)
Al2−Si1	2.548(2)	2.5504(8)	2.5499(9)
Al1−Si1−Al1	115.09(9)	115.06(3)	115.02(3)
2Al1−Si1−Al2	113.97(5)	114.066(19)	114.07(2)
2Al1−Si1−Al1	85.67(6)	85.50(2)	85.48(2)
Al2−Si1−Al1	138.88(8)	138.97(3)	139.03(3)
2Al1−Si2−Al2	121.74(4)	121.845(17)	121.852(18)
Al2−Si2−Al2	112.50(8)	112.37(3)	112.41(3)
Al1−Si2−Al2	135.27(9)	135.22(3)	135.26(3)
2Al2−Si2−Al2	75.63(6)	75.53(2)	75.45(2)
Si1−Al1−Si1	115.09(9)	115.07(3)	115.02(3)
2Si1−Al1−Si2	115.80(5)	115.76(2)	115.79(2)
2Si1−Al1−Si1	94.34(6)	94.50(2)	94.52(2)
Si2−Al1−Si1	117.71(9)	117.54(3)	117.48(3)
Si2−Al2−Si2	112.51(8)	112.37(3)	112.41(3)
2Si2−Al2−Si2	104.37(6)	104.47(2)	104.55(2)
Si2−Al2−Si1	108.79(6)	108.74(2)	108.69(2)
Si2−Al2−Si1	118.04(8)	118.06(3)	117.97(3)

Figure 2a−c illustrates the structure of $BaAl_2Si_2$ in the *Cmcm*, *I*4/*mmm*, and *Pnma* space groups, respectively. Many of the important features and crystallographic details of the *Pnma* structure type have been discussed previously;[22,26,32,41] only a concise description will be given here. The most important interatomic distances and angles are presented in Table 3. $BaAl_2Si_2$ forms a 3D network of Si and Al atoms that form large cavities in which Ba atoms reside. Ba is in a 7-fold coordination with respect to Si, with Ba−Si distances ranging from 3.2713(6) to 3.5975(5) Å (distances here and later from 10 K X-ray data). There are nine Al atoms surrounding each Ba, arranged in a capped trigonal prismatic configuration. The Ba−Al distances range from 3.3593(7) to 3.8175(7) Å. Both Si1 and Si2 have distorted tetrahedral coordination (although Si2 is not as distorted) by Al with Si−Al distances between 2.5048(5) and 2.5661(9) Å. The closest Si−Si and Al−Al distances are 3.7246(8) and 3.1155(9) Å, respectively. This structure can be thought of as distorted Al_2Si_2 layers connected by two Al−Si bonds, one at 2.5661(9) Å (Figure 1a, dotted black line) and the other at 2.5494(9) Å (Figure 1a, solid black line). In this structure, the Si and Al atoms are distinctly identified as occupying different sites. This is also the case for the isostructural phase α-$BaAl_2Ge_2$, in which Al and Ge are readily distinguishable and found to occupy different sites. As reported by Yamanaka et al.,[31] $BaAl_2Si_2$ also crystallizes in the space group *Cmcm* and forms similar Al_2Si_2 layers that are connected

(41) Iglesia, J. E.; Steinfink, H. *Z. Kristallogr.* **1975**, *142*, 398.

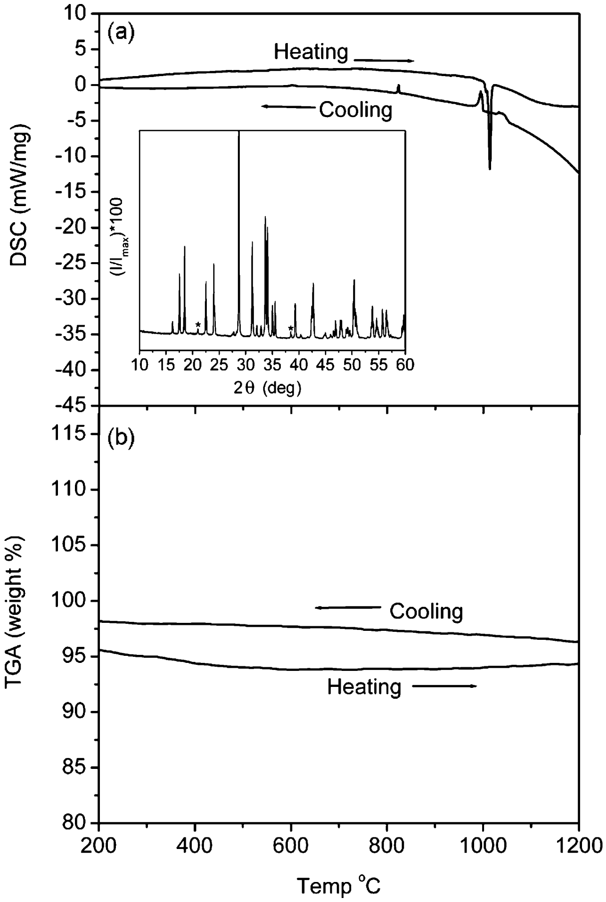

Figure 3. (a) DSC (mV mg^{-1}) traces as a function of temperature for $BaAl_2Si_2$. Data were obtained by heating at a rate of 4 K min^{-1} under argon. The inset displays the powder X-ray diffraction pattern of $BaAl_2Si_2$ after DSC measurement (* = additional phase). (b) TGA (wt %) traces as a function of temperature for $BaAl_2Si_2$.

by M−M bonds of 2.542(4) Å, where M = Al or Si, because Al and Si could not be distinguished for this phase.[31]

In comparison to α-$BaAl_2Ge_2$,[26] $BaAl_2Si_2$ shows shorter interatomic distances, as well as a reduced-volume unit cell. $BaAl_2Si_2$ is air stable and does not react with water, whereas α-$BaAl_2Ge_2$ is reported to be air and water sensitive.[26] This may be caused by the stronger covalent or metallic bonding in $BaAl_2Si_2$ or perhaps the growth of a thin surface-oxidation layer that protects the crystal. Figure 3a and 3b shows the DSC and TGA traces, respectively, for $BaAl_2Si_2$. α-$BaAl_2Ge_2$ is reported to have a structure transition at 827 °C, whereas Figure 3a shows no evidence of a structure transition for $BaAl_2Si_2$ (*Pnma*) The DSC traces presented in Figure 3a indicate that $BaAl_2Si_2$ melts (endotherm) at ∼1014 °C, which is close to the melting point of 1027 °C reported for $BaAl_2Si_2$ (*Cmcm*). Two exotherms are observed when the melt is cooled. One exotherms is broad, from ∼1054 to ∼1027 °C, and the other is sharp at ∼995 °C, indicating the recrystallization of $BaAl_2Si_2$. There is one additional exotherm in the cooling cycle at ∼824 °C which does not have a corresponding endotherm in the heating cycle. This indicates that $BaAl_2Si_2$ does not recrystallize as a single phase, which is also confirmed by X-ray powder diffraction taken after the DSC scan (inset of Figure 3a). It is important to note that there was no weight loss or gain observed in the TGA as shown in Figure 3b, indicating that the additional exotherms cannot be attributed to oxidation or vaporization.

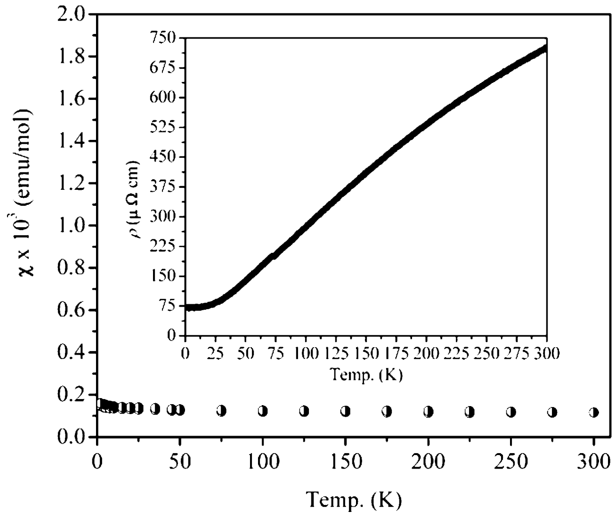

Figure 4. Temperature dependence of the susceptibility for $BaAl_2Si_2$. The inset shows the temperature dependence of the resistivity for $BaAl_2Si_2$.

Figure 4 shows the resistivity and magnetic susceptibility as a function of temperature. The resistivity and magnetic susceptibility are consistent with metallic character and is not immediately apparent when considering simple electron counting formalisms. In the Zintl formalism, the structure can be viewed as Ba^{2+} and $(Al^{3+})_2(Si^{4+})_2$ (16 e$^-$ total), where the Ba donates its electrons to the framework to charge compensate. In $BaAl_2Si_2$, Si and Al are both tetrahedrally coordinated. Si with four valence electrons has no need for extra electrons, but Al needs one more electron to achieve the same configuration as Si, giving the following charge compensation according to the Zintl−Klemm formalism: $Ba^{2+}(Al^-)_2(Si^0)_2$. This simple analysis suggests that $BaAl_2Si_2$ should be a semiconductor and is inconsistent with the temperature dependence of the electrical resistivity as shown in Figure 4, as well as the temperature-dependent magnetic susceptibility (inset of Figure 4) for $BaAl_2Si_2$ at 1 T, which exhibits Pauli paramagnetic behavior, characteristic of a metal.

However, many AB_2X_2 structures that crystallize in the well-studied $CaAl_2Si_2$ ($P\bar{3}m1$)[13] structure type exhibit metallic conductivity whether they are electrovalent, in the Zintl formalism, at 16 e$^-$ total, like $CaAl_2Si_2$, or not, like $YbAl_2Si_2$, which has a total of 17 e$^-$.[19−21,42] The metallic conductivity has been theoretically explored by Kranenberg et al. for the series AAl_2Si_2 and AAl_2Ge_2 where A = alkaline-earth or rare-earth atoms.[19,20] Their results showed that the metallic conductivity is a result of the electronic band structure.[19,20] More specifically, the metallic state arises only if the electronegativity difference between the atoms of the Al_2Si_2 or Al_2Ge_2 double layer is small enough to close the band gap between the valence band and conduction band.

Theoretical calculations have also been performed on the α-modification of $BaAl_2Ge_2$, which is isostructural to $BaAl_2Si_2$ in the *Pnma* space group.[26] Similar to the $CaAl_2Si_2$

(42) Bobev, S.; Tobash, P. H.; Fritsch, V.; Thompson, J. D.; Hundley, M. F.; Sarrao, J. L.; Fisk, Z. *J. Solid State Chem.* **2005**, *178*, 2091.

structure, the DOS of α-$BaAl_2Ge_2$ does not show a band gap and exhibits metallic conductivity. Additionally, the Al−Ge bonding is described as 2-centered $2e^-$.[25] Since $BaAl_2Si_2$ (*Pnma*) and α-$BaAl_2Ge_2$ are isostructural, the Al−Si bonding in $BaAl_2Si_2$ (*Pnma*) should be similar to the Al−Ge bonding in α-$BaAl_2Ge_2$. For the $CaAl_2Si_2$ type ($P\bar{3}m1$), Kranenberg et al. presented the idea that the electronegativity difference between Al and Si is small enough to close the band gap between the valence and conduction band, resulting in metallic conductivity. Thus, the metallic conductivity is a result of the electronic structure and cannot be rationalized by simple electron counting. On the basis of theoretical calculations, Leoni et al. also confirmed that metallic conductivity of α-$BaAl_2Ge_2$ is a result of electronic structure. Therefore, it can be proposed that the metallic conductivity found in $BaAl_2Si_2$ (*Pnma*) is a result of electronic structure and simple electron counting cannot rationalize the metallic properties.

Acknowledgment. The authors gratefully acknowledge Dr. Alexandra Navrotsky (Department of Chemistry and Thermochemistry Facility and NEAT ORU, University of California Davis) for use of the Scintag powder diffractometer. This work was supported by the National Science Foundation (Grant DMR-0600742), and C.L.C. acknowledges a Tyco Electronics Foundation Fellowship in functional materials. Work at Argonne National Laboratory was supported by the U.S. DOE, Basic Energy Sciences, Materials Sciences, under Contract DE-AC-02-06CH11357.

Supporting Information Available: Additional crystallographic data for $BaAl_2Si_2$ in CIF format. This material is available free of charge via the Internet at http://pubs.acs.org.

IC070078H